ORTRES 624
30 October 2003 Disk used
ARTICLE IN PRESS
No. of Pages 9, DTD = 4.3.1

ELSEVIER

Journal of Orthopaedic Research xxx (2003) xxx–xxx

Journal of Orthopaedic Research

www.elsevier.com/locate/orthres

Recruitment of mesenchymal stem cells and expression of TGF-β1 and VEGF in the early stage of shock wave-promoted bone regeneration of segmental defect in rats

Yeung-Jen Chen [a], Tilmann Wurtz [b], Ching-Jen Wang [c], Yur-Ren Kuo [d], Kuender D. Yang [e], Hue-Chen Huang [e], Feng-Sheng Wang [e,*]

[a] *Department of Orthopedic Surgery, Chang Gung University, Linkou, Taiwan*
[b] *University of Paris 7, Institut des Cordeliers, Inserm E110, France*
[c] *Department of Orthopedic Surgery, Chang Gung Memorial Hospital, Kaohsiung, Taiwan*
[d] *Department of Plastic and Reconstructive Surgery, Chang Gung Memorial Hospital, 123 Ta-Pei Road, Niao-Sung, Kaohsiung 833, Taiwan*
[e] *Department of Medical Research, Chang Gung Memorial Hospital, 123 Ta-Pei Road, Niao-Sung, Kaohsiung 833, Taiwan*

Received 17 March 2003; accepted 3 October 2003

Abstract

Extracorporeal shock wave (ESW) treatment has recently been established as a method to enhance bone repair. Here, we reported that ESW-promoted healing of segmental defect via stimulation of mesenchymal stem cell recruitment and differentiation into bone forming cells. Rats with a segmental femoral defect were exposed to a single ESW treatment (0.16 mJ/mm^2, 1 Hz, 500 impulses). Cell morphology and histological changes in the defect region were assessed 3, 7, 14, and 28 days post-treatment. Presence of mesenchymal stem cell was assayed by immuno-staing for RP59, a recently discovered marker, and also production of TGF-β1 and VEGF was monitored. ESW treatment increased total cell density and the proportion of RP59 positive cells in the defect region. High numbers of round- and cuboidal-shaped cells strongly expressing RP59 were initially found. Later, the predominant cell type was spindle-shaped fibroblastic cells, subsequently, aggregates of osteogenic and chondrogenic cells were observed. Histological observation suggested that bone marrow stem cells were progressively differentiated into osteoblasts and chondrocytes. RP59 staining was initially intense and decreased with the appearance of expression depended on the differentiation states of osteogenic and chondrogenic cells during the regeneration phase. Mature chondrocytes and osteoblasts exhibited only slight RP59 immuno-reactivity. Expression of TGF-β1 and VEGF-A mRNA in the defect tissues was also significantly increased ($P < 0.05$) after ESW treatment as determined by RT-PCR. Intensive TGF-β1 immuno-reactivity was induced immediately, whereas a lag period was observed for VEGF-A. Chondrocytes and osteoblasts at the junction of ossified cartilage clearly exhibited VEGF-A expression. Our findings suggest that recruitment of meseoblasts at the junction of ossified cartilage clearly exhibited mesenchymal stem cells is a critical step in bone reparation that is enhanced by ESW treatment. TGF-β1 and VEGF-A are proposed to play a chemotactic and mitogenic role in recruitment and differentiation of mesenchymal stem cells.

Keywords: Mesenchymal stem cell; Fracture healing; RP59; TGF-β1; VEGF-A; Shock wave

Introduction

Repair of fracture proceeds in a sequence of chondrogenesis, osteogenesis and remodeling that ultimately restores the integrity of the bone and its biomechanical characteristics. In normal fracture healing, mesenchymal stem cells differentiate into osteoblasts and chondrocytes to form a fracture callus that calcifies extracellular matrix and serve as scaffold for bone formation [5,47]. Nonunion, a failure of healing process, is evident when new bone fails to bridge a defect or when loose fibrous tissues or fibrocartilage develops [18]. Although preexisting osteoblasts may be involved in the repair to a limited extent, the differentiation of pluripotential mesenchymal stem cells into osteoblasts and chondral cells is regarded as a critical step in the formation of bony and cartilaginous tissues in defect [2]. Previous studies have reported that bone formation in the fracture defect could be achieved by introducing bone-inductive mate-

* Corresponding author. Tel.: +886-7-731-7123x8876.
E-mail address: wangfs@ms33.hinet.net (F.-S. Wang).

0736-0266/$ - see front matter © 2003 Orthopaedic Research Society. Published by Elsevier Ltd. All rights reserved.
doi:10.1016/j.orthres.2003.10.005

rials, indicating that responsive stem or progenitor cells are present in the defect. These cells can differentiate into bone and cartilage when appropriate osteogenic stimulation and microenvironment are provided [1,14, 23,35].

Extracorporeal shock waves (ESW) are generated by high voltage spark discharge under water. This causes an explosive evaporation of water, producing high-energy acoustic waves. By focusing the acoustic waves with a semi-ellipsoid reflector, the waves can be transmitted to a specific tissue site [29]. ESW have been found beneficial for the healing process of nonunion, acute fracture and calcified tendinitis [25,32,39,40]. It has been scintographically and sonographically implicated that local blood flow and metabolism of bone and Achilles tendon in rabbits were affected by ESW treatment [26,31]. However, cellular and biochemical mechanisms by which ESW enhance healing of fracture remains to be determined. We have earlier demonstrated that ESW could enhance osteogenic differentiation of mesenchymal stem cells in vitro as well as bony union of segmental defect in rats, indicating that the microenvironment of the defect is responsive to physical ESW stimulation [41–44].

The regulation of callus formation during fracture repair is mediated by the coordinate expression of growth factors [10]. Transforming growth factor-beta 1 (TGF-β1), one of abundant growth factors in bone matrix, has shown to be involved in regulating differentiation of osteoblast and production of extracellular matrix protein in the physical stimulation of fracture healing [11,33]. Also, vascular endothelial growth factor (VEGF) produced in the callus microenvironment takes an important part in the angiogenic process during fracture healing [16,37]. We therefore hypothesize that ESW treatment promotes bone regeneration through influx of mesenchymal stem cells into the defect, followed by differentiation matrix forming cells types. Cells in the defect region may be triggered by ESW to enhance production of angiogenesis and cell differentiation factors.

The purpose of present study was to investigate the recruitment of mesenchymal stem cells and histomorphological changes in a segmental femoral defect subjected to ESW treatment. We also elucidate whether physical ESW promotion of bone regeneration is linked to increase in TGF-β1 and VEGF expression.

Materials and methods

Segmental defect model

All studies were approved by the Institutional Animal Care and Use Committee of Chang Gung Memorial Hospital, Taiwan. Three-month-old Sprague-Dawley rats (National Experimental Animals Production Center, Taipei, Taiwan) were caged in pairs and maintained on rodent chow and water ad libitum. Rats were anesthetized by an intraperitoneal injection of pentobarbital sodium (50 mg/kg; Nembutal® sodium, Abbott Laboratories, IL, USA). A segmental femoral defect in each rat was operated as previously described [44]. Briefly, a four-hole AO/ASIF mini-plate was positioned on the anterolateral femoral shaft after stripping off the periosteum. The proximal and distal holes were drilled and tapped with 1.5-mm bicortical screws. A 5-mm long, full thickness disk of cortical and cancellous bone was resected from the middle of the diaphysis with a saline-cooled burr. The fixation plate was stabilized using a 0.45-mm Kirschner wire engaged with the trabecular bone in the proximal femoral diaphysis (Fig. 1). The wound was closed in layers. Chloromycinetin (10 mg/kg, intraperitoneal injection) and analgesia (0.02 mg/kg bupenorphine, subcutaneous injection; Reckitt and Colman Pharmaceutical Inc., Richmond, VA, USA) were administered for 2 days. Animals were allowed unrestricted post-operative activity and weight-bearing as tolerated. All rats gained weight during the study period. Anterposterior radiographs were taken using a mammography system (35 kV, 80 mAs, film to focus distance 50 cm; Lorad M-IV, Varian Inc., Salt Lake, UT, USA) post-operatively at 2-week intervals [44].

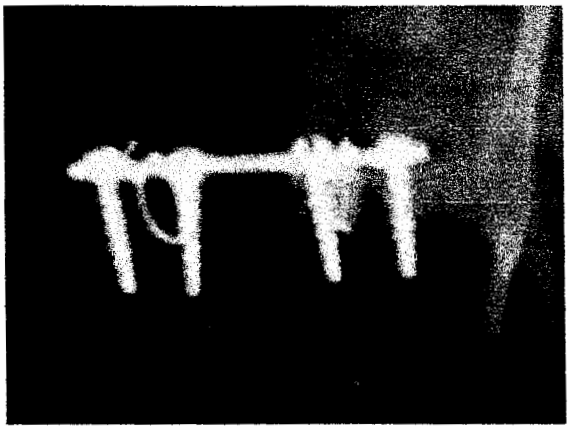

Fig. 1. Representative radiograph of segmental femoral defect in rats. Left femurs were subjected to osteotomy as described in Materials and methods. Radiographs were taken 12 weeks post-operatively.

ESW treatment

Each rat with a segmental defect was re-anesthetized 12 weeks post-operatively and placed in a supine position with all four limbs stabilized in extension. A single ESW treatment (0.16 mJ/mm² energy flux density; EFD, 500 impulses, 1 Hz; Ossatron® HMT High Medical Technologies GmbH, Kreuzlingen, Switzerland) was employed at the fracture site medially under flowscopy guidance. Each ESW treatment lasted 10 min. The ultrasound transmission gel (Pharmaceutical Innovations Inc, New Jersey, USA) was used as contact medium between the ESW apparatus and skin.

Experimental design

Sixty-four rats with segmental defects were randomly divided into ESW and control groups. All animals were re-anesthetized 12 weeks post-operatively. Thirty-two rats were given ESW treatment. Rats was killed using an overdose of intraperitoneal pentobarbital sodium 3 days ($n = 8$), 7 days ($n = 8$), 14 days ($n = 8$), 28 days ($n = 8$) after ESW treatment. The remaining 32 rats received no ESW treatment and were used as controls. Eight rats were killed at each time point as for the ESW group. Four femurs were dissected to harvest callus, and four for histological assessment. Calluses were cleaned of surrounding tissue, snap-frozen in liquid nitrogen and stored at −80 °C until RNA extraction.

RT-PCR

Calluses were ground with a mortar and pestle under liquid nitrogen and RNase-free conditions. Total RNA was extracted with Tri reagent containing monophasic solution of guanidine thiocyanate and phenol (Sigma Chemical Inc., St. Louis, MI, USA). A total of 1 μg RNA was reversely-transcribed (RT) using 0.5 mg/ml oligo(dT) primer, reverse transcription buffer, 10 mM dNTP mix and AMV reverse transcriptase (Promega Corporation, Madison, WI, USA), followed by PCR using rat gene-specific primers: TGF-β1 (sense) (5′-GCT GAA CCA AGG AGA CGG AAT-3′), TGF-β1 (antisense) (5′-GAG CTG TGC AGG TGT TGA GC-3′) (204-base pair expected); VEGF-A (sense) (5′-CTG TGC AGG CTG CTG TAA GG-3′); VEGF-A (antisense) (5′-GTT CCC GAA ACC CTG AGG AG-3′) (230-base pair expected); β-actin (sense) (5′-AGT ACC CCA TTG AAC ACG GC-3′), β-actin (antisense) (5′-TTT TCA CGG TTA GCC TTA GG-3′) (168-base pair expected). The RT-PCR cycling parameters were set as follows: the RT reaction at 50 °C for 2 min, 60 °C for 30 min; and 95 °C for 5 min; followed by 40 cycles of PCR reactions at 94 °C for 20 s and 60 °C for 1 min. The PCR products were electrophoresed on a 1.5% agarose gel containing ethidium bromide and visualized by UV-induced fluorescence. All signals were quantified by scan densitometry and the final result was obtained by calculating the TGF-β1/β-actin or VEGF-A/β-actin ratio. The stimulation factor was calculated by dividing the signal from the ESW sample by that of the respective control sample.

Immuno-histochemistry

Femurs were fixed in 4% buffered paraformaldehyde for 48 h and decalcified in PBS-buffered 10% EDTA. Decalcified tissues were embedded in paraffin. Bone specimens were longitudinally cut into 5-μm sections and transferred to poly-lysine-coated slides for conventional hematoxylin-eosin, alcain blue or alizarin red staining (Sigma Chemicals Inc, St. Louis, MO, USA) to distinguish fibrous, cartilaginous and bony tissues. Immuno-reactivity in specimens was demonstrated using a horseradish peroxidase (HRP)-3′-, 3′-diaminobenzidine (DAB) cell and tissue staining kit (R & D Systems, Inc., Minneapolis, MN, USA) according to the manufacturer's instructions. For immuno-localization of mesenchymal stem cells and early recruitment stages, antibodies against RP59, a protein in bone marrow cells and young osteoblasts were used [21,46]. To identify osteoblsts, chondrocytes and fibroblasts, sections were immuno-stained for bone alkaline phosphatase, osteocalcin (Developmental Studies Hybridoma Bank, University of Iowa, IA, USA) and prolyl 4-hydroxylase (Dako A/S, Glostrup, Denmark). Sections were also immuno-stained for TGF-β1 and VEGF-A (Upstate Biotechnology, Lake Placid, NY, USA). Sections were further incubated with biotinylated secondary antibodies with streptavidin conjugated to HRP, followed by chromogen solution and counterstaining with hematoxylin. Sections were dehydrated and mounted. Sections without primary antibodies were enrolled as negative controls for the immuno-staining.

Histomorphometric assessment

Five areas within the segmental defects from three sections obtained from four rats were randomly selected using a Zeiss Axioskop 2 plus microscope (Carl Zeiss, Gottingen, Germany). Areas (3 mm^2) containing positive immuno-stained cells were analyzed. Three random images of 0.75 mm^2 from each area (3 mm^2) were then taken under 400× magnifications. All the images of each specimen were captured using a Cool CCD camera (SNAP-Pro c.f. Digital kit; Media Cybernetics, Sliver Spring, MD, USA). The number of the hematoxylin-stained nucleus in each image was counted using an Image-Pro® Plus image-analysis software (Media Cybernetics, Sliver Spring, MD, USA) as previous described [24]. The number of positive immuno-labeled cells and total cells in each area were calculated. A professional pathologist, blinded to the treatment regimen performed measurement on all sections.

Statistical analysis

All values were expressed as mean ± standard error. Wilcoxson test was used to evaluate difference between the sample of interest and its respective control. For analysis time course, multiple ANOVA was used. A P value of <0.05 was considered significant.

Results

Animal model

All animals were operated successfully and survived during the experiment. Animals in both groups ambulated freely within 5 days post-operatively. All the wounds healed without infection, and there was no failure of fixation. Segmental gaps in both groups were obvious on radiographs 12 weeks post-operatively (data not shown). ESW treatment did not induce skin hemorrhage, ecchymosis, swelling or impair ambulation.

Histology

Segmental defects initially filled with loose fibrous connective tissue and skeletal muscle that had collapsed into the defects. Many fibroblasts and blood vessel were observed in the gap of both groups. The segmental defect underwent progressive mesenchymal aggregation and hypertrophied chondrogenesis 7 days after ESW treatment (Fig. 2A). Subsequently intensive intramembrane and endochondral ossification in the defect tissue was observed 14 days after ESW treatment (Fig. 2B). A large area of cartilage bridging the fracture gap was gradually replaced by bony tissue and reunited to be hard callus. Bone remodeling of the defect end was still in process 28 days after ESW treatment (Fig. 2C). Segmental defect of the control group displayed fibrous tissue and limited cartilage formation throughout the study period (not shown).

RP59 expression and cell morphology

RP59 has been identified in bone marrow cells with the capacity to differentiate into osteoblasts [46]. We further used antibodies against RP59 to identify the mesenchymal stem cells during bone formation in the segmental defect. In the absence of the primary antibody, no immuno-staining was visible. Cells positive for RP59 expression exhibited brown immuno-staining in the cell periphery and cytoplasm. Most of these cells were located adjacent to the cellular tissue of the defect region, at endosteal surfaces and in the medullar cavity. In the ESW groups, both a significantly higher cell density and relatively more RP59 positive cells were noted (Table 1). The peak effect of ESW in terms of RP59 positive cells was detected 14 days after treatment. In the control group, the number of RP59 positive cells was similar throughout the study period.

Cells expressing RP59 were further morphologically categorized into round- and cuboidal-shaped cells, ver-

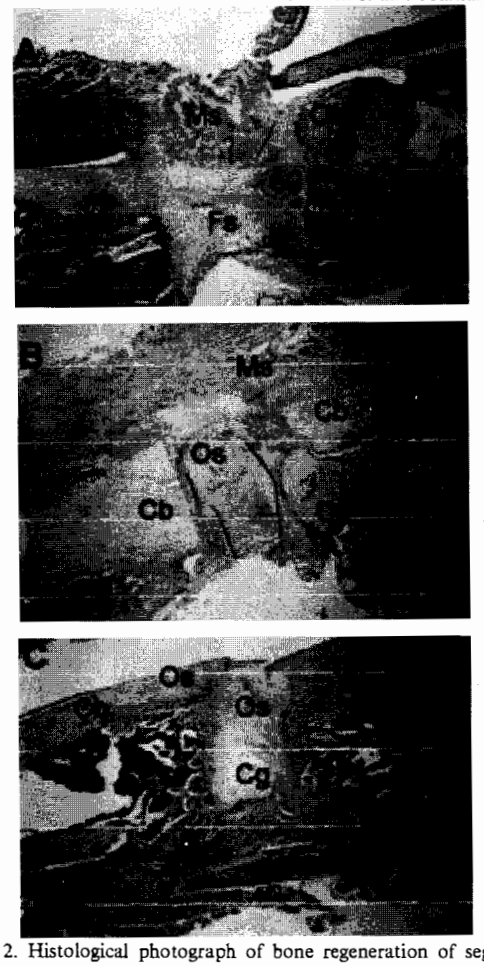

Fig. 2. Histological photograph of bone regeneration of segmental femoral after ESW treatment. (A) The defect is filled with fibrous connective tissue and muscular tissue. Cell aggregate, hypertrophic cartilage and ossified tissue were observed at 7 days after ESW treatment. (B) Intramembrane and endochondral ossification appeared in defect 14 days after treatment. (C) The defect is bridged by newly formed osseous tissue and hypertrophic cartilage. The bone remodeling of both defect ends is still in process. Specimens were stained with conventional hematoxylin-eosin and observed in magnification = 15×. Ag: Cell aggregate; Cb: cortical bone; Cg: cartilage; Fs: fibrous tissue; Ms: muscular tissue; Os: Ossified tissue. Bar scale = 2 mm.

sus spindle-shaped fibroblasts. Major cell morphology and extracellular matrix changes in the segmental defects were observed 3 days after ESW treatment. Round and cuboidal-shaped cells intensively expressing RP59 successively appeared in the center of the defect. Intermediates between round cells and dense extracellular matrix associated spindle-shaped cells were observed, suggesting differentiation of stem cells into fibroblasts (Fig. 3A). In the control sections, relatively few, either round- or spindle-shaped RP59 positive cells were distributed in loose fibrous connective tissue in the entire defect area of defect and at all time point (Fig. 3B). Spindle-shaped and elongated fibroblastic cells aligned along the axis of bone. In addition to fibroblastic cells, a further dramatic aggregation of RP59 positive cells into a more rounded appearance was observed after ESW treatment (Fig. 3C). In control sections, fibroblasts adjacent to fibrous tissue displayed very weak RP59 expression (Fig. 3D). We further used antibodies against prolyl 4-hydroxylase to differentiate fibroblasts and spindle-shaped mesechymal stem cells. Spindle-shaped RP59 positive cells did not express prolyl 4-hydroxylase (Fig. 3E), whereas fibroblsts in fibrous tissue appeared strong prolyl 4-hydroxylase immuno-expression (Fig. 3F). Seven days after ESW treatment, the rounded cells subsequently aggregated. Dense matrix formed around the aggregate that was stainable by alcain blue staining. Cell aggregates subsequently developed into cartilage-like structures expressing little RP59 (Fig. 3G). At the same time, few fibroblastic RP59 positive cells appeared in the fibrous tissue in the control sections (Fig. 3H). Fourteen and twenty-eight days after ESW, flat-shape osteoblastic-like cells with slight RP59 expression appeared adjacent to ossified tissue (Fig. 3I). In the control group, fibroblastic cells in fibrous tissue expressed RP59 only slightly (Fig. 3J). Expression of RP59 decreased upon differentiation into osteoblastic and chondroid cells. Table 2 summarizes the location and strength of RP59 expression in the defect after ESW treatment. Round- and cuboidal-shaped cells, as well as elongated fibroblastic cells at fibrous tissue displayed intensive RP59 expression. Spindle-shape fibroblastic cells around cell aggregated showed intermediate RP59 immuno-reactivity. Chondroid cells and osteoblastic cells displayed only slight RP59 expression. Mesenchymal stem cells, chondral, and osteoblastic cells did not express prolyl 4-

Table 1
Temporal changes in number of total cells and cells expressing RP59 in segment defect

Days after ESW	Total cells			RP59 cells		
	ESW[a]	Control[b]	*P*-value	ESW	Control	*P*-value
3	652 ± 96[c]	374 ± 68	0.019	304 ± 78	98 ± 23	0.005
7	916 ± 114	312 ± 89	<0.001	583 ± 91	92 ± 20	<0.001
14	1234 ± 264	383 ± 97	<0.001	833 ± 124	89 ± 19	<0.001
28	1113 ± 226	388 ± 69	<0.001	574 ± 102	103 ± 25	<0.001

[a] Rats with a segmental femoral defect were given a single ESW treatment (0.16 mJ/mm², 1 Hz, 500 impulses).
[b] Rats with a segmental defect received no ESW treatment.
[c] Data are mean ± SEM calculated from five segmental defect of areas from 3 sections of 4 rats.

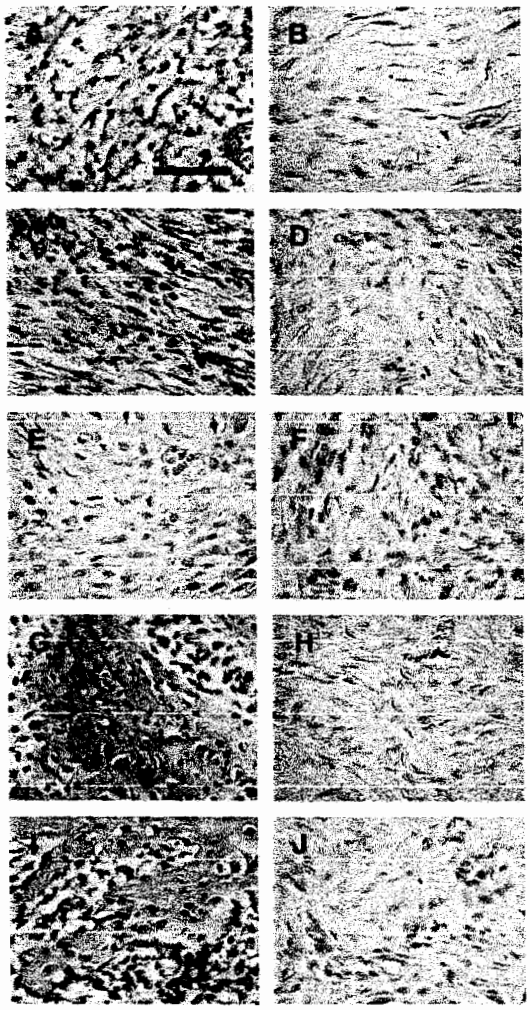

Fig. 3. Immuno-histochemical detection of RP59 and prolyl 4-hydorxylase in cells of the segmental defect region. (A) Many round and cuboidal cells expressing RP59 are present in the fibrous tissue after ESW treatment 3 days after ESW treatment. (B) Few round- and cuboidal-cells expressing RP59 distributed in fibrous and cellular tissue in the control groups. (C) Fibroblasts expressing RP59 along bone ends appear elongated 3 days after ESW treatment. (D) Fibroblastic slightly expressed RP59 filled the fibrous tissue in the controls. (E) RP59-stained fibroblasts weakly expressed prolyl 4-hydroxylase in ESW group. (F) Fibroblasts in the control group strongly expressed prolyl 4-hydroxylase. (G) Cells at newly formed cartilaginous tissue displayed slight RP59 expression. (H) Cells at fibrous tissue slightly expressed RP59 in controls (I) Cells at new developed bony tissue appeared slight RP59 expression 14 days after ESW treatment. (J) Cells at fibrous tissue slightly expressed RP59 in controls. The positive immuno-stained cells showed brown color, all cell nuclei appear blue because of hematoxylin counterstain. Specimens were observed in magnification = 400× and bar scale = 100 μm. (For interpretation of the references in colour in this figure legend, the reader is referred to the web version of this article.)

hydroxylase. Fibroblasts expressing prolyl 4-hydroxylase did not expression bone alkaline phosphatase and osteocalcin throughout the study period.

Osteogenic potential

Presence of bone alkaline phosphatase and osteocalcin was tested as indicators for the osteogenic potential. In both groups, cells expressing strong RP59 at fibrous tissue displayed slightly bone alkaline phosphatase expression (Fig. 4A and B). In the ESW groups, cells adjacent to the cell aggregates, expressing intermediate RP59, displayed intensive bone alkaline phosphatase immuno-reactivity (Fig. 4C). Mature osteoblasts with low RP59 in osseous tissue exhibited clear osteocalcin immuno-staining (Fig. 4E). In control sections, limited amount of cells at segmental defect area appeared slight bone alkaline phosphatase and osteocalcin expressions (Fig. 4D and F). The results indicated that cells with intensive RP59 expression were mainly mesenchymal cells and immature osteoblasts in early stages of differentiation. Cells at segmental defect subjected to osteogenic differentiation following ESW treatment.

TGF-β1 and VEGF-A expression

Experiments were conducted to investigate whether recruitment of mesenchymal stem cells after receiving ESW treatment could be linked to TGF-β1 and VEGF-A. In fact, TGF-β1 mRNA expression increased significantly ($P < 0.05$) in defect tissue at day 3 after ESW treatment and persisted to day 28 (Fig. 5). In contrast, VEGF-A mRNA expression in the defect tissue increased later 28 days after ESW treatment (Fig. 5). Table 3 summarizes the changes in cells numbers expressing TGF-β1 and VEGF-A. Three and seven days after ESW, immuno-staining revealed intensive TGF-β1 presence in mesenchymal stem cells at fibrous tissue sites and of fibroblasts in aggregated mesenchymal sites (Fig. 6A). In control sections, cells at segmental defect appeared slightly TGF-β1 expression (Fig. 6B). Fourteen and twenty-eight days after ESW treatment, chondral cells at the cartilaginous tissue and osteoblastic cells adjunct to the ossified tissue also displayed intensive TGF-β1 expression (Fig. 6C). In control groups, cells at the defect displayed weakly TGF-β1 expression (Fig. 6D). Mesenchymal stem cells at the fibrous tissue sites contained little VEGF-A. Chondral cells and osteoblastic cells at the newly formed cartilage and bone tissues exhibited intensive VEGF expression. Furthermore, vascularization appeared at the junction of cartilaginous and ossified tissues and exhibited strong VEGF-A immuno-staining 28 days after ESW treatment (Fig. 6E). In the control group, segmental defects were largely filled with fibrous tissue and few fibroblastic cells exhibited little VEGF-A signal (Fig. 6F).

Table 2
Spatial expression of RP59, prolyl 4-hydroxylase (P4Hase), bone alkaline phosphatase (APase) and osteocalcin (OCN) in segmental defect after receiving ESW treatment

Cell morphology	Location	Days	Immuno-reactivity			
			RP59	P4Hase	APase	OCN
Round cells	Fibrous tissue	3–7	+++	–	+	–
Spindle fibroblasts	Fibrous tissue	3–7	+++	–	+	–
Round cells	Cell aggregate	7–14	++	–	++	+
Spindle fibroblasts	Cell aggregate	7–14	++	–	+++	–
Round cells with lacuna	Osseous tissue	14–28	+	–	+	+++
Round cells with lacuna	Cartilage	14–28	+	–	–	–
Fibroblasts	Fibrous tissue	3–28	–	+++	–	–

+++: Intensive immuno-reactivity, ++: Intermediate immuno-reactivity, +: Slight immuno-reactivity, –: No immuno-reactivity.

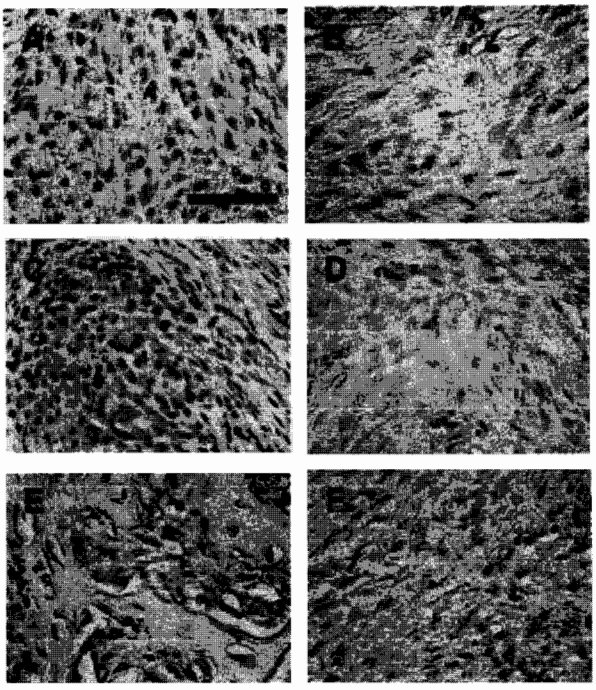

Fig. 4. Immuno-expression of bone alkaline phosphatase and osteocalcin expression in cells of the segmental defect region. (A and B) Round-shaped cells at cellular tissue appeared slight bone alkaline phosphatase expression in both ESW and control groups. (C) Cells adjunct to bone matrix displayed intensive bone alkaline phosphatase expression. (D) Cells at fibrous tissue in controls appeared slight bone alkaline phosphatase expression. (E) Cells at new developed bony tissue appeared intensive osteocalcin immuno-reactivity. (F) Cell at the fibrous tissue in controls displayed slight osteocalcin expression. Specimens were observed in magnification = 400× and bar scale = 100 μm.

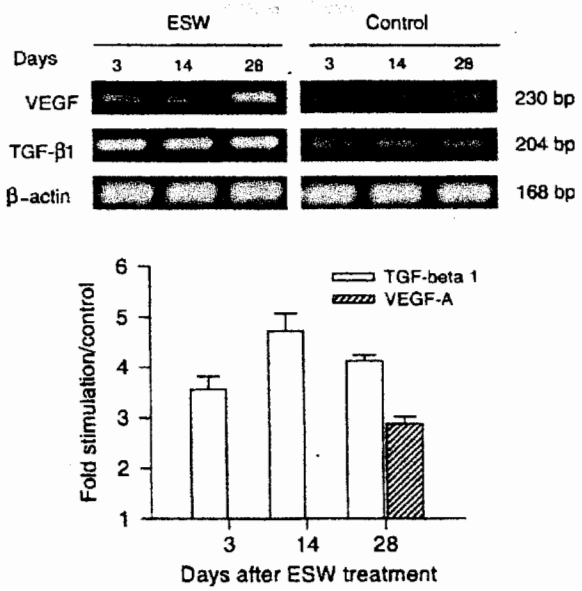

Fig. 5. Expression of TGF-β1 and VEGF-A mRNA in defect tissue. Significant increases in TGF-β1 expression were noted in ESW at all three time points. An evident up-regulation of VEGF-A mRNA expression was detected 28 days after treatment. The levels of TGF-β1 and VEGF-A mRNA expression in the segmental defect with and without ESW treatment were determined using RT-PCR assay.

Discussion

In normal bone model, ESW potentially causes detachment of periosteum from bone and hematoma, as well as altered blood flow and bone metabolism in rabbits [8,26]. These effects may enhance recruitment and proliferation of marrow-, muscle- and periosteum-derived osteogenic progenitor cells to the segmental defect. Our histological analysis suggests that mesenchymal stem cells adjacent to the segmental defect were subject to three consecutive events: intensive recruitment and proliferation, chondrogenic and osteogenic differentiation. ESW treatment promoted bone regeneration by stimulation of recruitment and differentiation of mesenchymal stem cells.

Segmental defects have been used as models of nonunion formation because they tend to form fibrous connective tissue during the healing process [1,14,23,35]. Rats with diaphyseal fracture of long bones have been reported to heal uneventfully within 8–12 weeks [12,19]. In this study, all segmental defects are radiographically visible 12 weeks post-operatively, suggesting that segmental defect provides as an excellent model for elucidating molecular and cellular changes in ESW-promoted bone regeneration of nonunion.

Table 3
Temporal changes in number of cells expressing TGF-β1 and VEGF-A in segment defect of ESW and control groups

Expression	Days	ESW[a]	Control[b]	P-value
TGF-β1	3	363 ± 63[c]	95 ± 16	0.023
	7	685 ± 112	101 ± 19	0.011
	14	867 ± 186	107 ± 16	<0.001
	28	912 ± 179	98 ± 18	<0.001
VEGF-A	3	102 ± 17	106 ± 14	0.569
	7	112 ± 21	113 ± 13	0.456
	14	429 ± 92	108 ± 14	0.022
	28	582 ± 106	114 ± 17	0.017

[a] Rats with a segmental femoral defect were given a single ESW treatment (0.16 mJ/mm², 1 Hz, 500 impulses).
[b] Rats with a segmental defect receiving no ESW treatment.
[c] Data are mean ± SEM calculated from five segmental defect of areas from 3 sections of 4 rats.

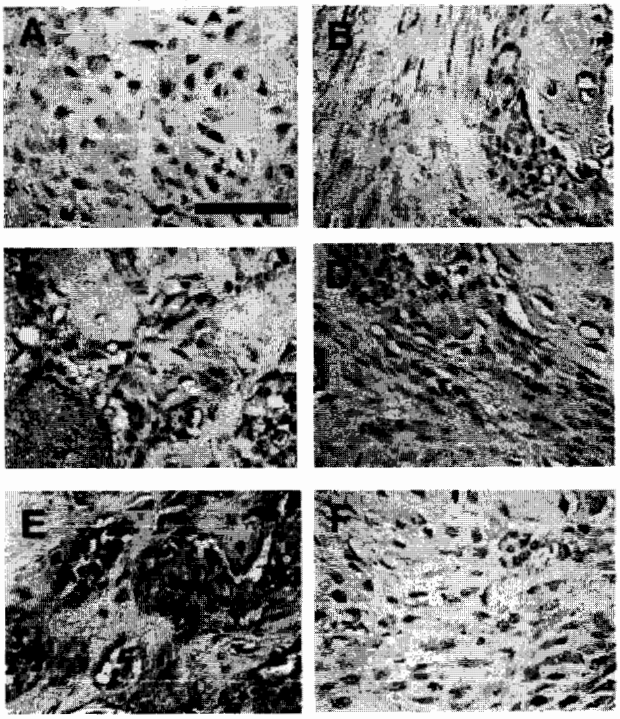

Fig. 6. Immuno-histochemical staining of TGF-β1 and VEGF-A after ESW treatment. (A) mesenchymal stem cells at fibrous tissue and fibroblastic cells at hypercellular tissue in ESW groups displayed intensive TGF-β1 expression. (B) Cells at fibrous and fibrocartilaginous tissues in controls showed slight TGF-β1 expression. (C) Immature chondral cells and osteoblasts at cartilaginous and osseous tissues in ESW group appeared intensive TGF-β1 expression. (D) Cells at fibrous and fibrocartilaginous tissue in controls displayed slight TGF-β1 expression (E) Cells at the junction of newly developed cartilage and bone tissues in ESW groups displayed intensive VEGF-A expression. (F) Cells at fibrocartilagous tissue appeared slight VEGF-A expression. The positive immuno-stained cells showed brown color. Specimens were observed in magnification = 400× and bar scale = 100 μm. (For interpretation of the references in colour in this figure legend, the reader is referred to the web version of this article.)

In contrast to previous studies demonstrating high-energy ESW (0.5 and 0.9 mJ/mm² EFD) damaged bone tissue in rabbits [8,26], we showed that ESW treatment (0.16 mJ/mm² EFD) did not induce side effects in rats. We speculate the discrepancy that influence of ESW on bone tissue depends on EFD and experimental animals. Intensive mesenchymal stem cell recruitment and progressive differentiation into cartilaginous and bony tissue is the most prominent findings of ESW treatment for segmental defect. As usual during healing of segmental defects, fibrous tissue and skeletal muscle with vessel filled the gap, whereupon typical bone morphogenesis preceded, including mesenchymal aggregation, hypertrophic chondrogenesis and intramembrane/endochondral ossification. Proliferation and differentiation of mesenchymal stem cells are critical for the development of a medullar callus that unites the fractured bone in advance of the deposition of osseous repair tissue in the fracture gap [5]. We have recently found that RP59 was induced in the early mesoderm of rat embryos and was suppressed during ensuing differentiation of many cell types, but maintained in young osteoblasts [21]. We provide here the first evidence that many cells expressing RP59 are capable to differentiate into osteogenic cells displaying bone alkaline phosphatase and osteocalcin immuno-reactivity for bone formation. However, also chondrocytes in the defect arose from stem cells, as judged by their residual content of RP59. The osteogenic capacity of mesenchymal stem cells seem not to be limited to a few bone marrow cells, but widespread, since ESW treatment grossly augmented the number of RP59 positive cells contributing to bone formation. This finding emphasizes the plasticity of mesenchymal stem cells to adjust the direction of differentiation according to external conditions [28]. The limitation of this study is that morphological assessment is not a specific method for identifying mesechymal stem cells. Few previous studies of bone repair have monitored mesenchymal stem cells of rat because specific markers for such cells are scarce. We have further employed antibodies against RP59, bone alkaline phosphatase and osteocalcin to specifically distinguish cuboidal- and spindle-shaped osteogenic precursor cells in the segmental defect. It is not presently known whether mature fibroblasts can differentiate into chondrocytes or osteoblasts. We verify that fibroblasts expressing prolyl 4-hydroxylase do not express bone alkaline phosphatase and osteocalcin. Our findings indicate that fibroblasts may not be responsible for osteogenesis and chondrogenesis during bone repair.

In both ESW and control rats, mesenchymal stem cells preexisted in the defect tissue to the same extent. Recruitment and differentiation of mesenchymal stem cells were enhanced after ESW treatment. A previous study has indicated that survival, proliferation and collagen I biosynthesis in human cancellous bone cells are altered following ESW [22]. These suggest that mesenchymal stem cells can perceive and respond to acoustic

energy and pressure released by ESW and translate the stimulus into a biochemical response leading to cellular adaptation. Raising the availability and differentiation capacity of mesenchymal stem cells in segmental defect tissue is proposed as an explanation for the clinical success of ESW procedure. Both stimulations of cell migration and of local cell proliferation can improve the availability of cells. Our previous studies ex vivo and in vitro also support the hypothesis that ESW treatment promotes mesenchymal stem cell growth and osteogenic differentiation [41–43]. It is unknown at present how acoustic energy and pulsed high pressure released by ESW is translated into biological signals which promoting recruitment and osteogenic differentiation of mesenchymal stem cell. Bone tissue responded to physical stimulation could elevate release of anabolic molecules of bone tissue [10,34]. A previous study has reported that ESW-augmented bone formation in periosteum is probably via induction of substance P [27]. We recently have found that bone morphogenetic proteins (BMPs) are actively involved in ESW-promoted healing of segmental defects [44]. Osteogenic transcription factor (Cbfa1/Runx2) and Indian hedgehog (Ihh) are further candidates to mediate chondrogenic and osteogenic differentiation of mesenchymal stem cells after ESW treatment [43].

The observed effects of ESW may be mediated by TGF-β1 and VEGF-A, regulating migration and differentiation of mesenchymal stem cells and subsequent bone formation. TGF-β1 is a potential chemotactic stimulator for bone cells and promotes biosynthesis of extracellular matrix [30]. This growth factor actively regulated chondrogenesis and osteogenesis in bone regeneration [6,9,45]. The results of RT-PCR and immuno-histochemistry demonstrated that TGF-β1 expression was elevated after ESW treatment. Furthermore, intensive TGF-β1 expression was observed in mesenchymal stem cells, chondral and osteoblastic cells of the ESW groups throughout the study period. We suggest that TGF-β1 is likely to play a mitogenic role in mesenchymal stem cell growth. Angiogenesis plays a critical role in successful bone regeneration, causing up-regulation of blood flow to the fracture in the healing process [15,16]. VEGF is an important modulator that regulates vascularization and endochondral ossification during fracture healing [13,38]. In contrast to previous study demonstrating vascularization occurred in fracture hematoma in the early stage of acute fracture healing [36], histological findings in this study showed that hematoma was completely resolved and fibrous tissue with blood vessels was observed in the osteotomy gap of both groups 12 weeks after surgery. While we did not perform any studies on vascularization, an increased VEGF-A expression was much more latter than TGF-β1 in the defect after ESW treatment. We speculate that biological response raised by ESW stimulation may depend on the model system used, cell and tissue types. Chua and his co-workers have reported that TGF-β1 is involved in regulating VEGF-A expression of osteoblasts [7]. VEGF-A expression in maturation stages of osteochondral cells was significantly increased 28 days after ESW treatment. These findings support previous studies that VEGF is responsible for hypertrophied cartilage neovascularization [4,38]. In our study, intensive TGF-β1 and VEGF-A expression in defect tissue suggests that their production is directly or indirectly promoted by physical stimulation provided by ESW treatment, and that TGF-β1 and VEGF are actively involved in recruitment and differentiation of mesenchymal stem cells. Each factor has a distinct temporal expression pattern, suggesting different roles in bone regeneration of segmental defect. Together, our research provides evidence that ESW treatment is a noninvasive method for extension of mesenchymal stem cells in bone repair. This method can, for many defects, be a alternative biophysical strategy for tissue engineering and transplantation of bone marrow as a source for mesenchymal stem cells [3,17,20,35].

Acknowledgements

This work was supported in part by grants from National Health Research Institute, Taiwan [NHRI-EX92-9128EI (F.S.W.)] and a grant [NSC-90-2314-B-182A-045 (Y.J.C.)] from the National Science Council, Taiwan.

References

[1] Boyan BD, Caplan AI, et al. Osteochondral progenitor cells in acute and chronic canine nonunions. J Orthop Res 1999;17:246–55.

[2] Bruder SP, Fink DJ, Calpan AI. Mesenchymal stem cells in bone development, bone repair, and skeletal regeneration therapy. J Cell Biochem 1994;56:283–94.

[3] Bruder SP, Kurth AA, et al. Bone regeneration by implantation of purified culture-expanded human mesenchymal stem cells. J Orthop Res 1998;16:155–62.

[4] Carlevaro MF, Cermeli S, Cancedda R, Descalzi Cancedda F. Vascular endothelial growth factor (VEGF) in cartilage neovascularization and chondrocyte differentiation: auto-paracrine role during endochondral bone formation. J Cell Sci 2000;113:59–69.

[5] Chakkalakal DA, Strates BS, Mashoof AA, et al. Repair of segmental bone defects in the rats: an experimental model of human fracture healing. Bone 1999;25:321–32.

[6] Cho TJ, Gerstenfeld LC, Eihorn TA. Differential temporal expression of members of the transforming growth factor β superfamily during murine fracture healing. J Bone Miner Res 2002;17:513–20.

[7] Chua CC, Hamdy RC, Chua BH. Mechanism of transforming growth factor-beta1-induced expression of vascular endothelial growth factor in murine osteoblastic MC3T3-E1 cells. Biochem Biophys Acta 2000;1497:69–76.

[8] Delius M, Draenert K, Al Diek Y, Draenert Y. Biological effects of shock waves: in vivo effect of high energy pulses on rabbit bone. Ultra Med Biol 1995;21:1219–25.
[9] D'Angelo M, Sarment DP, Billings PC, Pacific M. Activation of transforming growth factor β in chondrocytes undergoing endochondral ossification. J Bone Miner Res 2001;16:2339–47.
[10] Eihorn TA, Majeska RJ, Rush EB, Levine PM, Horowitz MC. The expression of cytokine activity by fracture callus. J Bone Mine Res 1995;10:1272–81.
[11] Eingartner C, Coerper S, Fritz J, et al. Growth factors in distraction osteogenesis. Int Orthop 1999;23:253–9.
[12] Ekeland A, Engesaeter LB, Langeland N. Influence of age on mechanical properties of healing fractures and intact bones in rats. Acta Orthop Scand 1982;53:527–32.
[13] Ferguson C, Alpern E, Miclau T, Helms JA. Does adult fracture repair recapitulate embryonic skeletal formation? Mech Develop 1999;87:57–66.
[14] Friedlaender GE, Perry CR, Cole JD, et al. Osteogenic protein-1 (bone morphogenetic protein 7) in the treatment of tibia nonunion. J Bone Joint Surg Am 2001;83:S151–8.
[15] Gerber HP, Vu TH, Ryan AM, et al. VEGF couples hypertrophic cartilage remodeling, ossification and angiogenesis during endochondral bone formation. Nat Med 1999;5:623–8.
[16] Glowacki J. Angiogenesis in fracture healing. Clin Orthop 1998;355:S82–9.
[17] Hannouche D, Petite H, Sedel L. Current trends in the enhancement of fracture healing. J Bone Jt Surg Br 2001;83:157–64.
[18] Hayda RA, Brighton CT, Esterhai JL. Pathophysiology of delayed healing. Clin Orthop 1998;355:31–40.
[19] Hietaniemi K, Peltonen J. Paavolainen An experimental model for nonunion in rats. Injury 1995;26:681–6.
[20] Hunt TR, Schwappach JR, Anderson HC. Healing of segmental defect in the rat femur with use of an extract from a cultured human osteosarcoma cell-line (Saos-2). J Bone Jt Surg Am 1999;78:41–8.
[21] Kruger A, Ellestrom C, Lundmark C, Christersson C, Wurtz T. RP59, a marker for osteoblast recruitment, is also detected in primitive mesenchymal cells, erythroids and megakaryocytes. Develop Dyn 2002;223:414–8.
[22] Kusnierczak D, Brocai DR, Vettel U, Loew M. Effect of extracorporeal shockwave administration on biological behavior of bone cells in vitro. Z Orthop Ihre Grenzgeb 2000;138:29–33.
[23] Lieberman JR, Daluiski A, Stevenson S, et al. The effect of regional gene therapy with bone morphogenetic protein-2-producing bone-marrow cells on the repair of segmental femoral defects in rats. J Bone Jt Surg Am 1999;81:905–17.
[24] Li G, White G, Connolly C, Marsh D. Cell proliferation and apoptosis during fracture healing. J Bone Miner Res 2002;17:791–9.
[25] Loew M, Daecke W, Kusnierczak D, Rahmanzadeh M, Ewerbeck V. Shock-wave therapy is effective for chronic calcifying tendinitis of the shoulder. J Bone Jt Surg Br 1999;81:861–7.
[26] Maier M, Milz S, Tischer T, et al. Influence of extracorporeal shock-wave application on normal bone in an animal model in vivo. J Bone Joint Surg Br 2002;84:592–9.
[27] Maier M, Averbeck B, Milz S, Refior HJ, Schmitz C. Substance P and prostaglandin E_2 release after shock wave application to the rabbit femur. Clin Orthop 2003;406:237–45.
[28] Magli MC, Levantini E, Giorgetti T. Developmental potential of somatic stem cells in mammalian adults. J Hemat Stem Cell Res 2000;9:961–9.
[29] Ogden JA, Toth-Kischkat A, Schultheiss R. Principles of shock wave therapy. Clin Orthop 2001;387:8–17.
[30] Pfeilschifter J, Wolf O, Naumann A, Mundy GR, Ziegler R. Chemotactic response of osteoblastic like cells to TGF-β. J Bone Miner Res 1990;5:825–30.
[31] Rompe JD, Kirkpatrick CJ, Kullmer K, Schwitalle M, Kirschek O. Dose-related effects of shock waves on rabbits tendo Achillis: a sonographic and histological study. J Bone Joint Surg Br 1998; 80:546–52.
[32] Rompe JD, Rosendahl T, Schollner C, Theis C. High-energy extracorporeal shock wave treatment of nonunions. Clin Orthop 2001;387:102–11.
[33] Rosier RN, O'Keefe RJ, Hicks DG. The potential role of transforming growth factor in fracture healing. Clin Orthop 1998; 355:294–300.
[34] Salter DM, Wallace WHB, Robb JE, Caldwell H, Wright MO. Human bone cell hyperpolarization response to cyclic mechanical strain is mediated by an interleukin-1β autocrine/paracrine loop. J Bone Miner Res 2001;15:1746–55.
[35] Stevenson S, Cunningham N, Toth J, Davy D, Reddi AH. The effect of osteogenin (a bone morphogenic protein) on the formation in orthotopic segmental defects in rats. J Bone Joint Surg Am 1994;76:1676–87.
[36] Street J, Winter D, Wang JH, Wakai A, et al. Is human fracture hematoma inherently angiogenic? Clin Orthop 2000;378:224–37.
[37] Street J, Bao M, deGuzman L, et al. Vascular endothelial growth factor stimulates bone repair by promoting angiogenesis and bone turnover. Proc Nat Acad Sci USA 2002;99:9656–61.
[38] Villars F, Bordenave L, Bareille R, Amedee J. Effect of human endothelial cells on human bone marrow stromal cell phenotype: role of VEGF. J Cell Biochem 2000;79:672–85.
[39] Wang CJ, Chen HS, Chen CE, Yang KD. Treatment of non-union fracture of the long bone with shock waves. Clin Orthop 2001;387:95–101.
[40] Wang CJ, Huang HY, Chen HS, Pai CH, Yang KD. Effect of shock wave therapy on acute fractures of the tibia. A study in a dog model. Clin Orthop 2001;387:112–8.
[41] Wang FS, Yang KD, Chen RF, Wang CJ, Sheen-Chen SM. Extracorporeal shock wave promotes growth and differentiation of bone-marrow stromal cells towards osteoprogenitor associated with induction of TGF-β1. J Bone Jt Surg Br 2001;84:457–61.
[42] Wang FS, Wang CJ, Huang HJ, et al. Physical shock wave mediates membrane hyperpolarization and Ras activation for osteogenesis in human bone marrow stromal cell. Biochem Biophys Res Commun 2001;287:648–55.
[43] Wang FS, Wang CJ, Sheen-Chen SM, et al. Superoxide mediates shock wave induction of ERK-dependent osteogenic transcription factor (CBFA1) and mesenchymal cell differentiation toward osteoprogenitors. J Biol Chem 2002;277:10931–7.
[44] Wang FS, Yang KD, Kuo YR, et al. Temporal and spatial expression of bone morphogenetic proteins in shock wave-promoted healing of segmental defect in rats. Bone 2003;32:387–96.
[45] Weiss S, Baumgart R, Jochum M, Strasburger CJ, Bidlingmaier M. Systemic regulation of distraction osteogenesis: a cascade of biochemical factors. J Bone Miner Res 2002;17:1280–9.
[46] Wurtz T, Kruger A, Christersson C, Lundmark C. A new protein expression in bone marrow cells and osteoblasts with implication in osteoblast recruitment. Exp cell Res 2001;263:236–42.
[47] Yoo JU, Johnstone B. The role of osteochondral progenitor cells in fracture healing. Clin Orthop 1998;355:73–81.